American Mineralogist, Volume 95, pages 386–391, 2010

Gayite, a new dufrénite-group mineral from the Gigante granitic pegmatite, Córdoba province, Argentina

Anthony R. Kampf,[1,*] Fernando Colombo,[2] and José González del Tánago[3]

[1]Mineral Sciences Department, Natural History Museum of Los Angeles County, 900 Exposition Blvd., Los Angeles, California 90007, U.S.A.
[2]CONICET, Cátedra de Geología General, Facultad de Ciencias Exactas, Físicas y Naturales, Pabellón Geología, Universidad Nacional de Córdoba, Vélez Sarsfield 1611, (X5016GCA) Córdoba, Argentina
[3]Departamento de Petrología y Geoquímica, Facultad de Ciencias Geológicas, Universidad Complutense, 28040 Madrid, Spain

Abstract

Gayite, ideally $NaMn^{2+}Fe^{3+}_5(PO_4)_4(OH)_6 \cdot 2H_2O$, is a new member of the dufrénite group found at the Gigante granitic pegmatite, Punilla department, Córdoba province, Argentina. It is named for Hebe D. Gay (b. 1927), Professor Emeritus of Mineralogy of the National University of Córdoba (Argentina). The new mineral is monoclinic, space group $C2/c$, a = 25.975(3) Å, b = 5.1766(3) Å, c = 13.929(1) Å, β = 111.293(2)°, Z = 4. The strongest lines in the X-ray powder diffraction pattern are [d in Å, (I)]: 12.054 (33), 5.045 (60), 4.147 (37), 3.424 (71), 3.179 (100), 3.004 (33), 2.881 (42), 2.426 (36), 2.109 (39), 1.585 (50). It occurs associated with morinite, natrodufrénite, and quartz in cavities in massive apatite-(CaF), as clusters of tabular crystals up to 130 μm on edge dominated by {100}, with subordinate {20$\bar{1}$} and possibly also {110}, {111}, and {11$\bar{1}$}. Crystals display striations parallel to [010]. The mineral is greenish black with an olive green streak and vitreous luster. Thin tablets are transparent. Gayite is brittle, with perfect {100} cleavage and irregular fracture. Its Mohs hardness is 4 to 5. The measured density is 3.15(5) g/cm^3, and the calculated density is 3.241 g/cm^3. The mineral dissolves slowly in dilute HCl. Gayite is biaxial (+), α = 1.787(3), β = 1.792(3), γ = 1.806(3), $2V_{meas}$ = 60(5)°, $2V_{calc}$ = 62.1°; moderate dispersion, $r < v$; strong pleochroism, X (bluish-green) >> Z (orange) > Y (yellow); orientation Y = **b**, X ^ **a** = 48° in obtuse β. Analysis by electron microprobe (average of 28 analyses given in wt%) provided TiO_2 0.12, Al_2O_3 3.10, Fe_2O_3 41.95, MnO 5.97, MgO 0.08, CaO 0.23, ZnO 0.15, Na_2O 3.03, P_2O_5 32.73, and H_2O (calculated by stoichiometry) 10.31, total 97.67 wt%. The empirical formula, based on 24 O, is $(Na_{0.85}Ca_{0..02})_{\Sigma 0.87}(Mn^{2+}_{0.74}Fe^{2+}_{0.12}Mg_{0.02}Zn_{0.02}Ti^{4+}_{0.01})_{\Sigma 0.90}(Fe^{3+}_{4.47}Al_{0.53})_{\Sigma 5.00}(P_{4.03}O_{16})(OH)_6 \cdot 2H_2O$. The crystal structure (R_1 = 6.10%) shows gayite to be a member of the dufrénite group, along with dufrénite, natrodufrénite, matioliite, and burangaite. The structure is a framework consisting of $Fe^{3+}O_6$ octahedra, $Mn^{2+}O_6$ octahedra, and PO_4 tetrahedra with channels along the **b** axis containing Na atoms. The most unusual feature of the structure is an octahedral face-sharing Fe^{3+}-Mn^{2+}-Fe^{3+} trimer.

Keywords: Gayite, new mineral, dufrénite group, pegmatite phosphate, Córdoba, Argentina

Introduction

Phosphates from evolved granitic pegmatites, especially those where primary triphylite-lithiophilite has been altered by late hydrothermal solutions, include a great number of species and have been extensively studied, from structural and paragenetic perspectives (e.g., Moore 1973, 1982; Hawthorne 1998; Simmons et al. 2003). In contrast, those from less evolved pegmatites containing only triplite and apatite-group minerals as primary phases have received less attention, possibly because they are not as diversified.

During a detailed examination of hydrothermal phosphates from the Gigante pegmatite, a beryl-columbite-phosphate [triplite- and apatite-(CaF)]-bearing pegmatite located in central Argentina, we found crystals of a mineral that was initially identified as a member of the dufrénite group using powder X-ray diffraction. Subsequent studies proved it to be a new species. In this contribution, we document its physical and chemical attributes and report details of its crystal structure.

The new species is named gayite for Hebe Dina Gay (b. 1927), Professor Emeritus of Mineralogy of the National University of Cordoba (Argentina). Among the many accomplishments of Gay's 60-year career in teaching, research, and curation, is the leadership she provided as the curator of the University's Alfredo Stelzner Museum of Mineralogy and Geology since 1971, organizing and building its collection, almost without support, into one of Argentina's most important geological museums. Gay studied the pegmatites of the Punilla Department and especially their phosphate minerals, extensively. She was co-author of the description of benyacarite, a new mineral from the El Criollo pegmatite, a few kilometers east of the Gigante pegmatite.

Both the new mineral and its name have been approved by the Commission on New Minerals, Nomenclature and Classification of the International Mineralogical Association (IMA 2008-056).

* E-mail: akampf@nhm.org

Cotype material is deposited in the Natural History Museum of Los Angeles County, California (specimen no. 59843), and in the Museo de Mineralogía "Dr. Alfred Stelzner," Universidad Nacional de Córdoba, Argentina (specimen no. MS003278).

Occurrence

The type locality of gayite is the Gigante pegmatite, 18.45 km W-SW of the town of Tanti, Punilla department, Córdoba Province, Argentina (Lat. 31°24′31.0″S, Long. 64°46′19.6″W).

This pegmatite is an intragranitic body genetically related to the postorogenic Achala batholith (Fig. 1). This batholith, with an area of ca. 2500 km^2, is dominated by monzogranitic units emplaced at 7–10 km depth (Lira and Kirschbaum 1990; Baldo 1992). U-Pb SHRIMP ages range between 379(4) and 369(3) Ma (Rapela et al. 2008). These authors recognized six main facies, four of which are modally classified as monzogranite, one as granodiorite, and another as tonalite. They are calc-alkaline to alkaline-calcic and mostly peraluminous (the most abundant facies has an average Aluminum Saturation Index of 1.19, n = 46).

The Achala batholith is composed of granites that can be classified as aluminous A-type following the criteria proposed by Whalen et al. (1987) and King et al. (1997). Major and trace-element whole-rock compositions, the zircon age pattern, and Nd isotopic signatures suggest that the granites probably had a mixed origin, resulting from the combination of a juvenile, probably asthenospheric component, and melting of granites of Cambrian age (Rapela et al. 2008).

Pegmatites are common in this sector of the Achala batholith, and have been grouped as the Punilla district (Galliski 1999). One of the most characteristic features of these pegmatites is the ubiquitous presence of triplite-zwieselite, sometimes as masses reaching more than 2 m in diameter.

The Gigante pegmatite, emplaced in equigranular monzogranite, is a lensoidal body more than 100 m long by 40 m wide and at least 25 m deep (Latorre et al. 1990). It is zoned, with border, wall, and at least two intermediate zones. A distinct core has not been found. Very close to the main outcrop are two other outcrops that may be part of the same pegmatite.

The pegmatite is composed of the common rock-forming minerals in peraluminous bodies (quartz, plagioclase, potassic feldspar, muscovite, and biotite). Abundant accessory phases are beryl, columbite-group minerals (Fe- and Nb-rich), apatite-(CaF) and triplite, which occur mostly in the intermediate zones. Other less common species are ixiolite, microlite-group minerals,

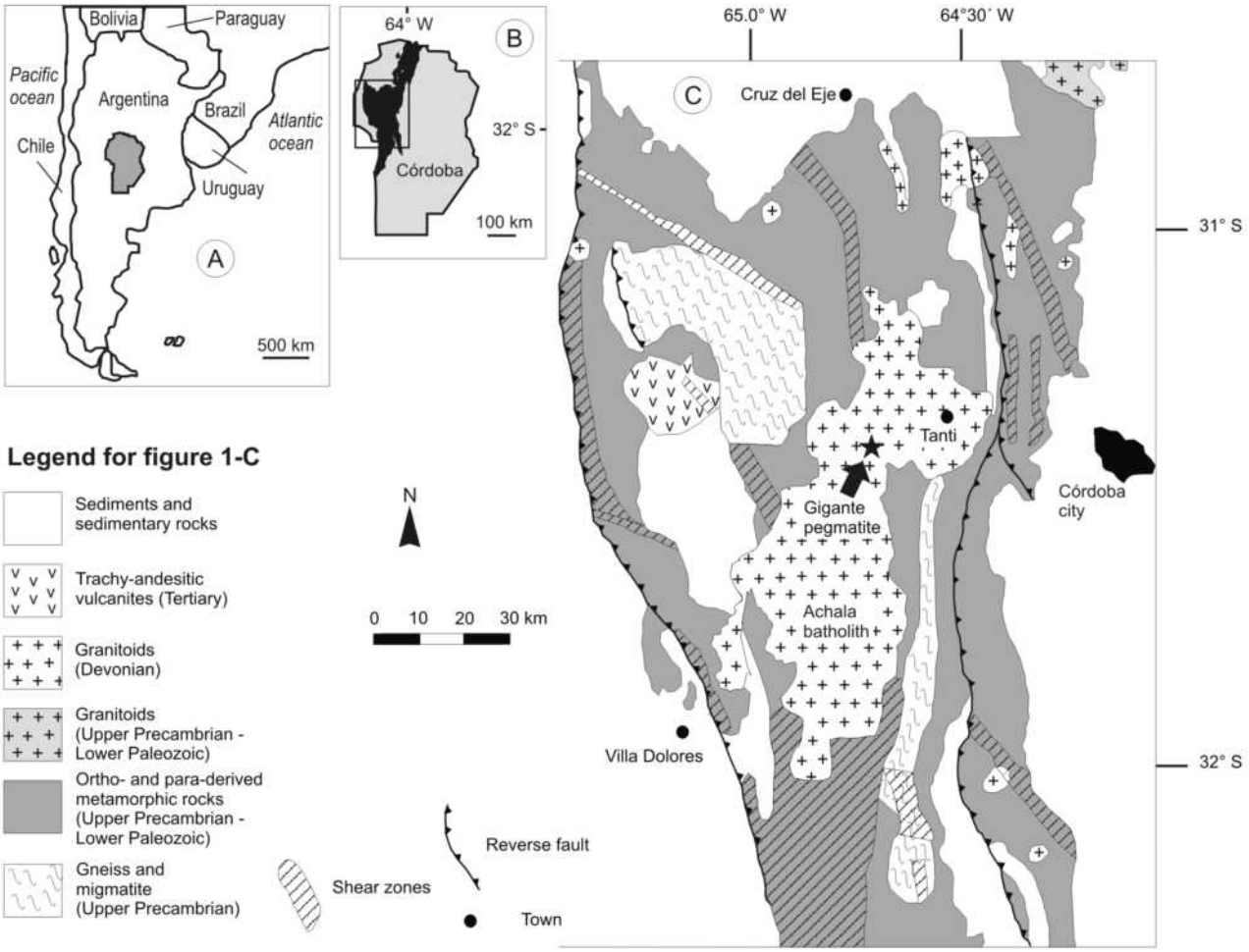

Figure 1. (**a**) Southern South America. Córdoba province is shaded gray. (**b**) Córdoba province, with the Pampean Ranges shown in black. The box marks the area expanded in **c**. (**c**) Geological map of the Achala batholith and the surrounding region. The map has been simplified from Martino (2003).

zircon, spessartine, carlhintzeite, uraninite, hematite, and ilmenite (Latorre et al. 1990; Galliski and Černý 2006). The Gigante pegmatite was mined using open-pit methods for quartz, potassic feldspar, beryl, and muscovite, for industrial uses. Currently it is abandoned and flooded.

The only sample known of gayite was found in the dumps. It consists of massive triplite and apatite-(CaF) with grains of pyrite, most of which have been oxidized. Gayite occurs in small vugs in apatite-(CaF), some of them left by altered pyrite, which are lined by grayish-white stout prisms and thin corroded crystals of apatite-(CaF) of hydrothermal origin. Pinkish tan spherules of morinite and salmon-colored crystals of quartz are also associated with gayite. One grain examined showed zoning with variable Mn/Fe ratios, some zones being gayite and others natrodufrénite.

In the same sample, but not in immediate association with the new mineral, are strengite, phosphosiderite, pyrite, chalcopyrite, digenite, and chalcocite. Other hydrothermal phosphates, including bermanite, childrenite/eosphorite, cyrilovite, fluellite, hentschelite, lacroixite, metatorbernite, and galliskiite (Kampf et al. 2010), also occur in the pegmatite.

Physical and optical properties

Gayite forms tabular crystals dominated by {100}, with subordinate {20$\bar{1}$}. No other forms are apparent, but the shape of the tablets suggests that some combination of the forms {110}, {111}, and {11$\bar{1}$} may also be present (Fig. 2). Crystals display striations parallel to [010]. No twinning was observed. Crystals reach 130 μm on edge and are often grouped, sometimes as curved, worm-like aggregates up to about 1 mm long composed of clusters of subparallel crystals.

The new mineral is transparent in thin tablets, greenish black with an olive green streak and has vitreous luster. It does not fluoresce under either SW or LW ultraviolet radiation. The Mohs hardness is 4 to 5 [scratches fluorite, but does not scratch apatite-(CaF)]. Gayite is brittle, with perfect {100} cleavage and irregular fracture. Parting was not observed. Visually it is very similar to dufrénite and can only be distinguished with certainty by chemical analyses or X-ray diffraction.

The density, measured using a Berman balance, is 3.15(5) g/cm^3, whereas the density calculated from the empirical formula is 3.245 g/cm^3 and that calculated from the formula based on the structure refinement is 3.226 g/cm^3. The difference could be due to air trapped in cavities present in the measured grains, which consisted of a mesh-works of intergrown crystals, or to inclusions of quartz and apatite-(CaF).

Gayite is biaxial (+); its indices of refraction, measured using a spindle stage in white light, are α = 1.787(3), β = 1.792(3), γ = 1.806(3). The measured 2V is 60(5)°, and the calculated 2V is 62.1°. It exhibits moderate dispersion, $r < v$. The optical orientation is Y = **b**, X ^ **a** = 48° in obtuse β. Pleochroism is strong with X (bluish-green) >> Z (orange) > Y (yellow).

The Gladstone-Dale compatibility index $1 - (K_P/K_C)$ as defined by Mandarino (1981) provides a measure of the consistency among the average index of refraction, calculated density, and chemical composition. For gayite, the compatibility index is 0.044, indicating good agreement among these data.

Chemical composition

Grains of gayite from four different vugs were mounted using epoxy resin on a glass slide, polished and coated with carbon. Chemical analyses were carried out by means of a JEOL JXA 8900M electron microprobe at the Centro de Microscopía Electrónica Luis Brú (Universidad Complutense de Madrid), operating in WDS mode, using 15 kV, 20 nA, and a beam diameter of 5 μm. Counting times were 20 s on peak and 10 s on the background, at each side of the peak. The standards used include kaersutite (for Ti, Mg and Ca), sillimanite (for Al), almandine (for Fe and Mn), albite (for Na), gahnite (for Zn), microcline (for K), and apatite-(CaF) (for P). H_2O content was not directly measured due to the paucity of material and the fact that gayite occurs intimately mixed with apatite-(CaF) and quartz. Instead, H_2O was calculated from the structure refinement (cf. Hawthorne and Grice 1990). The average of 28 analyses appears in Table 1. Other elements sought but not detected (at a 2σ level) and their standards were Si (460 ppm, albite), Cu (880 ppm, chalcopyrite), F (1360 ppm, apatite-CaF), and Cl (200 ppm, apatite-CaF).

The empirical formula, based on 24 O, is $(Na_{0.85}Ca_{0.02})_{\Sigma 0.87}(Mn^{2+}_{0.74}Fe^{2+}_{0.13}Mg_{0.02}Zn_{0.02}Ti^{4+}_{0.01})_{\Sigma 0.91}(Fe^{3+}_{4.47}Al_{0.53})_{\Sigma 5.00}(P_{4.03}O_{16})(OH)_6 \cdot 2H_2O$. Three structural sites, M1, M3, and M4, have similar sizes and clearly contain Fe^{3+} and Al. The empirical formula is based on full occupancy of these sites, with all remaining Fe assigned

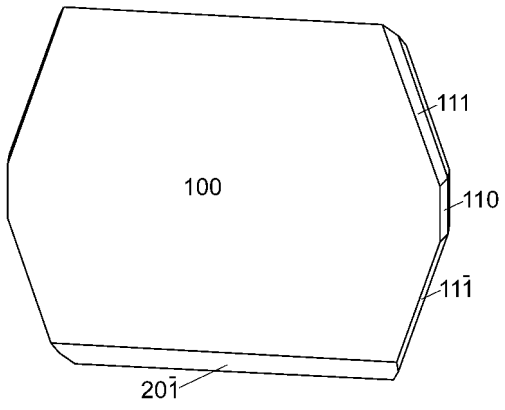

Figure 2. Crystal drawing of gayite (clinographic projection).

Table 1. Average results of 28 points of electron microprobe analyses of gayite

Constituent	wt%	Range	Stand. dev.	apfu	wt% in ideal formula
TiO_2	0.12	<0.08–0.28	0.09	0.01	
Al_2O_3	3.10	1.51–4.96	0.87	0.53	
Fe_2O_3*	41.95	38.40–44.18	1.43	4.47 Fe^{3+} + 0.12 Fe^{2+}	45.62
MnO	5.97	4.20–8.67	0.88	0.74	8.11
MgO	0.08	<0.03–0.24	0.06	0.02	
ZnO	0.15	<0.10–0.41	0.11	0.02	
CaO	0.23	0.11–0.46	0.09	0.02	
Na_2O	3.03	2.06–3.99	0.58	0.85	3.54
K_2O	0.00	<0.03–0.03	0.01	0.00	
P_2O_5	32.73	31.87–33.83	0.57	4.03	32.44
Subtotal	86.48	93.91–83.74	3.74		
H_2O†	10.22			6 OH + 2 H_2O	10.30
Total	97.58			10.82	100.00

* Assuming full occupancy of the M1, M3, and M4 sites by Al and Fe^{3+} with all remaining Fe assigned to the M2 site as Fe^{2+}, the Fe_2O_3 provided above can be reapportioned as Fe_2O_3 = 40.79 and FeO = 1.05 wt%.
† H_2O calculated from the crystal structure refinement.

to the M2 structural site as Fe^{2+}. The simplified formula is $NaMn^{2+}Fe^{3+}_5(PO_4)_4(OH)_6 \cdot 2H_2O$, which requires Na_2O 3.54 (wt%), MnO 8.11, Fe_2O_3 45.62, P_2O_5 32.44, H_2O 10.30, totaling 100.00 wt%.

Chemical homogeneity varied between analyzed crystals, as evidenced by backscattered electron images. Some grains are unzoned, whereas others show an intricate pattern with irregular or concentric zones. Some of these zones do not have enough Mn to dominate in the M2 site, so they are natrodufrénite. The mineral seems to be stable under the operating beam conditions used, and the polish is good (as seen on SEM images). The reason for the low analytical total is not readily apparent. Gayite dissolves slowly in dilute HCl.

X-RAY CRYSTALLOGRAPHY AND STRUCTURE REFINEMENT

Both powder and single-crystal X-ray diffraction data were obtained on a Rigaku R-Axis Spider curved imaging plate microdiffractometer utilizing monochromatized Mo$K\alpha$ radiation. The powder data are presented in Table 2.

The Rigaku CrystalClear software package was used for processing of the structure data. The SHELXL97 software (Sheldrick 2008) was used for the solution and refinement of the structure. The cation and oxygen sites reported by Moore (1970) for the dufrénite structure were used as a starting point. The large channel cation site, X, refined to full occupancy with Na. Metal atoms were assigned to the octahedral cation sites, M1, M2, M3, and M4, based upon bond distance and valence balance considerations. Fe^{3+} and Al were assigned to the smaller sites, M1, M3, and M4. Mn^{2+} and Fe^{2+} were assigned to the larger site, M2. The total occupancies of these sites were held at 1.0, while the individual occupancies by each cation were refined. With all non-hydrogen atoms located and refined including anisotropic displacement parameters at full occupancies, the R_1 (conventional R factor) converged to 6.10% for 675 reflections with $F_o > 4\sigma F$. Because gayite crystals occur in subparallel intergrowths, it was necessary to collect on a very small crystal fragment. The generally low intensities of the resulting data contributed to the rather high R-values, including R_{int} (Table 3). Hydrogen atoms could not be located; however, bond valence requirements indicate that O5, O8, and O11 are OH and O12 is H_2O. Four likely hydrogen bonds were identified based upon reasonable bond geometry, O-O bond distances, and bond valence considerations.

The details of the data collection and structure refinement are provided in Table 3. The final atomic coordinates and equivalent isotropic displacement parameters are in Table 4 and the anisotropic displacement parameters in Table 5. Selected interatomic distances are listed in Table 6 and bond valences in

TABLE 2. X-ray diffraction data for gayite

I_{obs}	d_{obs}	d_{calc}	hkl	I_{obs}	d_{obs}	d_{calc}	hkl
33	12.054	12.084	200*	8	2.300	2.306	$\bar{9}14$
10	6.865	6.834	$\bar{2}02$*			2.295	222
8	6.483	6.477	002*	5	2.236	2.237	$\bar{1}15$
9	6.031	6.042	400*	11	2.161	2.158	$\bar{12}$ 02
60	5.045	5.052	$\bar{1}10$*			2.159	$\bar{0}06$
13	4.841	4.833	$\bar{1}11$	39	2.109	2.108	$\bar{1}11$*
25	4.393	4.391	$\bar{3}11$*	29	2.069	2.069	$\bar{2}24$*
37	4.147	4.139	$\bar{1}12$*	18	2.013	2.016	$\bar{8}22$*
13	4.024	4.028	600			2.003	206
7	3.789	3.786	$\bar{4}02$*	24	1.9505	1.9493	$\bar{6}22$*
13	3.666	3.661	$\bar{5}11$*	7	1.8527	1.8534	$\bar{5}17$
		3.458	$\bar{2}04$	4	1.8074	1.8075	$\bar{11}$ 16
71	3.424	3.417	$\bar{3}13$*	13	1.7598	1.7540	$\bar{13}$ 15
		3.417	$\bar{4}04$	15	1.7305	1.7362	$\bar{6}08$
100	3.179	3.176	$\bar{5}13$*			1.7263	14 00
		3.166	$\bar{1}13$	11	1.6849	1.6867	$\bar{7}15$
33	3.004	3.000	$\bar{7}11$*			1.6864	$\bar{3}31$
42	2.881	2.882	$\bar{3}14$*	28	1.6580	1.6605	$\bar{8}26$*
		2.871	710			1.6562	$\bar{12}$ 22*
9	2.808	2.803	512	16	1.6137	1.6192	$\bar{0}08$
28	2.640	2.639	711*			1.6112	$\bar{16}$ 04
17	2.585	2.583	020	50	1.5848	1.5829	$\bar{2}26$*
6	2.500	2.501	404	4	1.5585	1.5571	$\bar{7}32$
		2.435	$\bar{5}13$*	9	1.5324	1.5303	$\bar{5}32$
36	2.426	2.416	$\bar{2}22$	19	1.4995	1.5002	$\bar{14}$ 22*
		2.416	$\bar{5}15$			1.5008	$\bar{12}$ 26
				17	1.4572	1.454	$\bar{3}19$

Notes: Reflection indexing based on intensities from structure data. Calculated d-spacings are based on the cell parameters refined from the powder data: a = 25.938(2), b = 5.1663(6), c = 13.902(2) Å, β = 111.286(8)°.
* Reflections used for cell refinement.

TABLE 3. Data collection and structure refinement details for gayite

Diffractometer	Rigaku R-Axis Spider with curved imaging plate
X-ray radiation / power	Mo$K\alpha$ (λ = 0.71075 Å) / 50 kV, 40 mA
Temperature	298(2) K
Empirical structural formula	$Na(Fe_{0.74}Al_{0.26})(Mn_{0.95}Fe_{0.05})(Fe_{1.53}Al_{0.47})(Fe_{1.78}Al_{0.22})(PO_4)_4(OH)_6 \cdot 2H_2O$
Space group	$C2/c$
Unit-cell dimensions	a = 25.975(3) Å
	b = 5.1766(4) Å
	c = 13.929(1) Å
	β = 111.293(2)°
Z	4
Volume	1745.1(3) Å^3
Density (for formula above)	3.226 g/cm^3
Absorption coefficient	4.910 mm^{-1}
F(000)	1541
Crystal size	0.06 × 0.05 × 0.01 mm
θ range	3.14–20.81°
Index ranges	$-25 \le h \le 25$, $-5 \le k \le 4$, $-13 \le l \le 13$
Reflections collected / unique	6919 / 901 [R_{int} = 0.132]
Reflections with $F_o > 4\sigma F$	675
Completeness to θ = 27.46°	99.0%
Refinement method	Full-matrix least-squares on F^2
Parameters refined	166
GoF	1.081
Final R indices [$F_o > 4\sigma F$]	R_1 = 0.0610, wR_2 = 0.1503
R indices (all data)	R_1 = 0.0822, wR_2 = 0.1624
Largest diff. peak / hole	+1.26 / –0.54 e/A^3

Notes: $R_{int} = \Sigma|F_o^2 - F_o^2(\text{mean})|/\Sigma[F_o^2]$. GoF = $S = \{\Sigma[w(F_o^2 - F_c^2)^2]/(n-p)\}^{1/2}$. $R_1 = \Sigma||F_o| - |F_c||/\Sigma|F_o|$. $wR_2 = \{\Sigma[w(F_o^2 - F_c^2)^2]/\Sigma[w(F_o^2)^2]\}^{1/2}$. $w = 1/[\sigma^2(F_o^2) + (aP)^2 + bP]$ where a is 0.0967, b is 0, and P is $[2F_c^2 + \text{Max}(F_o^2, 0)]/3$.

TABLE 4. Atomic coordinates, occupancies, and equivalent isotropic displacement parameters (Å^2) for gayite

	x	y	z	Occ.	U_{eq}
Na	0.0000	–0.1704(15)	0.2500		0.034(2)
Fe1/Al1	0.0000	0.0000	0.0000	0.73/0.27(1)	0.029(1)
Mn2/Fe2	0.2500	0.2500	0.0000	0.93/0.07(1)	0.028(1)
Fe3/Al3	0.1531(1)	–0.0199(4)	0.1095(2)	0.76/0.24(2)	0.026(1)
Fe4/Al4	0.1397(1)	–0.2286(4)	0.3495(2)	0.87/0.13(2)	0.027(1)
P1	0.2165(2)	0.2614(7)	0.3309(3)		0.030(1)
P2	0.0785(2)	0.2707(7)	0.3918(3)		0.034(1)
O1	0.0879(4)	0.0548(17)	0.3239(7)		0.038(3)
O2	0.0775(4)	0.5317(17)	0.3391(7)		0.036(3)
O3	0.0227(4)	0.2278(18)	0.4024(7)		0.040(3)
O4	0.1241(4)	0.2720(18)	0.4986(7)		0.036(3)
O5	0.1687(4)	0.2285(16)	0.0105(7)		0.036(3)
O6	0.2074(4)	0.0108(17)	0.3822(7)		0.036(3)
O7	0.1987(4)	–0.5111(16)	0.3821(7)		0.031(3)
O8	0.1285(4)	–0.2671(17)	0.2010(7)		0.036(3)
O9	0.1777(4)	0.2548(16)	0.2188(7)		0.036(3)
O10	0.2241(4)	–0.2125(18)	0.1557(7)		0.034(3)
O11	0.0753(4)	0.1330(19)	0.0676(7)		0.038(3)
O12	0.0232(4)	–0.2897(17)	0.1075(7)		0.036(3)

Table 7. The observed and calculated structure factors and the CIF are on deposit[1].

GAYITE AND OTHER MEMBERS OF THE DUFRÉNITE GROUP

The dufrénite structure (Fig. 3) is a framework consisting of four different types of octahedra (M1, M2, M3, and M4) and two different PO_4 tetrahedra (P1 and P2) with channels along the **b** (5 Å) axis containing larger cations (X) in eightfold coordination. The M1 and M3 octahedra share only corners with other octahedra and tetrahedra, while the M2 and M4 octahedra form a face-sharing octahedral M4-M2-M4 trimer.

Five minerals share the dufrénite structure: dufrénite, natrodufrénite, gayite, burangaite, and matioliite (Table 8). Structure analyses have been performed on all except natrodufrénite [dufrénite by Moore (1970); burangaite by Selway et al. (1997); matioliite by Atencio et al. (2006)]. In each case, the smaller M1, M3, and M4 octahedral sites are all dominated by either Fe^{3+} or Al^{3+}, the larger M2 site is dominated by Fe^{2+}, Mn^{2+}, or Mg and

[1] Deposit item AM-10-009, CIF. Deposit items are available two ways: For a paper copy contact the Business Office of the Mineralogical Society of America (see inside front cover of recent issue) for price information. For an electronic copy visit the MSA web site at http://www.minsocam.org, go to the *American Mineralogist* Contents, find the table of contents for the specific volume/issue wanted, and then click on the deposit link there.

TABLE 5. Anisotropic displacement parameters (Å²) for gayite

Atom	U_{11}	U_{22}	U_{33}	U_{23}	U_{13}	U_{12}
Na	0.028(5)	0.046(5)	0.024(5)	0.000	0.007(4)	0.000
Fe1/Al1	0.032(2)	0.030(2)	0.021(2)	0.000(1)	0.008(2)	–0.001(2)
Mn2/Fe2	0.028(2)	0.025(2)	0.022(2)	–0.003(1)	0.001(2)	–0.002(1)
Fe3/Al3	0.030(2)	0.027(2)	0.019(2)	–0.001(1)	0.005(1)	0.001(1)
Fe4/Al4	0.033(2)	0.025(2)	0.020(2)	0.001(1)	0.006(1)	0.000(1)
P1	0.038(3)	0.023(2)	0.027(3)	0.000(2)	0.009(2)	0.002(2)
P2	0.037(3)	0.034(3)	0.028(3)	0.002(2)	0.010(2)	0.002(2)
O1	0.060(7)	0.025(6)	0.026(6)	–0.005(4)	0.014(5)	0.010(5)
O2	0.050(7)	0.032(6)	0.022(5)	0.014(4)	0.009(5)	0.000(5)
O3	0.036(7)	0.044(7)	0.033(6)	0.003(5)	0.003(5)	0.008(5)
O4	0.025(6)	0.045(7)	0.030(6)	0.002(4)	0.001(5)	0.003(4)
O5	0.045(7)	0.034(6)	0.022(6)	0.000(4)	0.003(5)	0.008(5)
O6	0.035(6)	0.040(6)	0.028(6)	–0.005(5)	0.006(5)	–0.002(5)
O7	0.043(6)	0.027(6)	0.021(6)	–0.002(4)	0.010(5)	–0.004(4)
O8	0.043(7)	0.045(7)	0.018(6)	0.007(4)	0.011(5)	–0.002(5)
O9	0.041(6)	0.037(6)	0.024(6)	–0.008(4)	0.006(5)	0.005(5)
O10	0.025(6)	0.040(6)	0.036(6)	0.003(4)	0.009(5)	0.006(4)
O11	0.033(6)	0.041(6)	0.036(6)	0.004(5)	0.007(5)	0.004(5)
O12	0.048(7)	0.037(6)	0.025(6)	0.008(4)	0.014(5)	–0.004(5)

TABLE 6. Selected bond distances (Å) for gayite

Na-O12(×2)	2.357(10)	M1-O11(×2)	1.963(9)	M2-O6(×2)	2.103(9)
Na-O1(×2)	2.434(10)	M1-O3(×2)	2.042(9)	M2-O7(×2)	2.170(9)
Na-O2(×2)	2.481(10)	M1-O12(×2)	2.049(9)	M2-O5(×2)	2.172(10)
Na-O3(×2)	2.862(11)	<M1-O>	2.029	<M2-O>	2.157
<Na-O>	2.534				
		M3-O4	1.952(9)	M4-O1	1.935(9)
P1-O10	1.492(9)	M3-O10	1.986(9)	M4-O8	1.992(9)
P1-O9	1.520(10)	M3-O9	2.010(9)	M4-O2	2.001(9)
P1-O7	1.532(9)	M3-O5	2.030(10)	M4-O7	2.046(9)
P1-O6	1.540(10)	M3-O11	2.048(9)	M4-O6	2.062(9)
<P-O>	1.521	M3-O8	2.064(9)	M4-O5	2.090(9)
		<M3-O>	2.028	<M4-O>	2.038
P2-O3	1.524(10)				
P2-O4	1.529(10)	H-bonds:		O5···O4	2.814(14)
P2-O2	1.533(9)			O8···O9	2.755(12)
P2-O1	1.541(9)			O12···O3	2.870(14)
<P-O>	1.532			O12···O8	2.570(14)

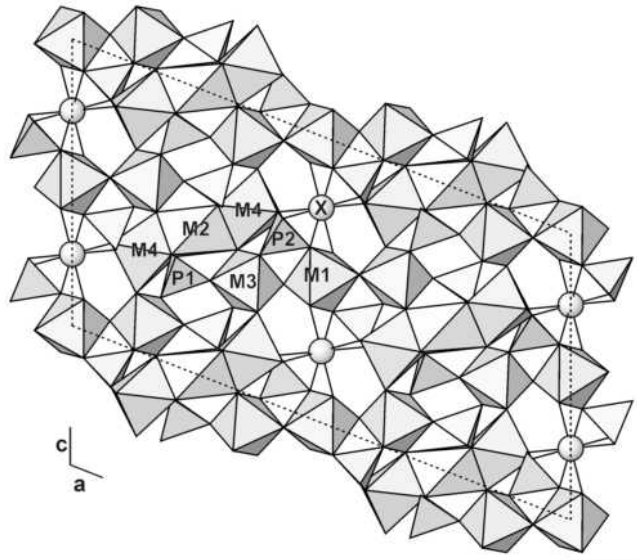

FIGURE 3. The dufrénite structure. The X cation site (Na or Ca), the M1, M2, M3, and M4 octahedra, and the P1 and P2 tetrahedra are labeled.

TABLE 8. Members of the dufrénite group

Name	Ideal formula	X	M2	M1,M3,M4
dufrénite	$Ca_{0.5}Fe^{2+}Fe^{3+}_5(PO_4)_4(OH)_6{\cdot}2H_2O$	Ca	Fe^{2+}	Fe^{3+}
natrodufrénite	$NaFe^{2+}Fe^{3+}_5(PO_4)_4(OH)_6{\cdot}2H_2O$	Na	Fe^{2+}	Fe^{3+}
gayite	$NaMn^{2+}Fe^{3+}_5(PO_4)_4(OH)_6{\cdot}2H_2O$	Na	Mn^{2+}	Fe^{3+}
burangaite	$NaFe^{2+}Al_5(PO_4)_4(OH)_6{\cdot}2H_2O$	Na	Fe^{2+}	Al
matioliite	$NaMgAl_5(PO_4)_4(OH)_6{\cdot}2H_2O$	Na	Mg	Al

TABLE 7. Bond valences for gayite

	O1	O2	O3	O4	O5	O6	O7	O8	O9	O10	O11	O12	$\Sigma_c v$
Na	0.180 $_{\times 2\rightarrow}$	0.159 $_{\times 2\rightarrow}$	0.057 $_{\times 2\rightarrow}$									0.222 $_{\times 2\rightarrow}$	1.234
M1			0.431 $_{\times 2\rightarrow}$								0.534 $_{\times 2\rightarrow}$	0.423 $_{\times 2\rightarrow}$	2.778
M2					0.352 $_{\times 2\rightarrow}$	0.425 $_{\times 2\rightarrow}$	0.354 $_{\times 2\rightarrow}$						2.262
M3				0.553	0.448			0.409	0.473	0.505	0.427		2.815
M4	0.598	0.501			0.394	0.425	0.443	0.513					2.873
P1						1.231	1.258		1.300	1.402			5.191
P2	1.228	1.255	1.286	1.269									5.037
H5				0.170	0.830								1.000
H8								0.810	0.190				1.000
H11											1.000		1.000
H12A			0.160									0.840	1.000
H12B								0.270				0.730	1.000
$\Sigma_a v$	2.006	1.914	1.934	1.992	2.024	2.080	2.056	2.002	1.963	1.907	1.961	2.215	

Note: Bond strengths from Brese and O'Keeffe (1991); hydrogen bond strengths from Ferraris and Ivaldi (1988), based on O-O distances; valence summations are expressed in valence units.

the X channel site is dominated by Ca (in ½ occupancy) or Na. Note that for natrodufrénite, virtually all Fe was provided as Fe^{3+} in the original description (Fontan et al. 1982) with the empirical formula given as $[Na_{0.63}(H_2O)_{0.35}Ca_{0.02}](Fe^{3+}_{0.67}Fe^{2+}_{0.05})(Fe^{3+}_{4.11}Al_{0.89})[(PO_4)_{3.80}(H_2O_4)_{0.20}][(OH)_{5.56}(H_2O)_{0.44}]\cdot 2H_2O$. However, considering the improbability that Fe^{3+} occupies the M2 site that shares faces with two adjacent Fe^{3+} octahedra, it is likely that more of the Fe in natrodufrénite is in the 2+ oxidation state and that the M2 site in natrodufrénite is dominantly occupied by Fe^{2+}.

Despite the differences in the M1, M3, and M4 sites, their strong tendencies toward occupancy by the same cation, either Fe^{3+} or Al, suggests that these sites should be grouped for purposes of defining species within the dufrénite group. Only considering Fe^{2+}, Mn^{2+}, and Mg as possible dominant constituents in the M2 site and Na and Ca in the X site, a total of 12 species are possible in the dufrénite group.

Reported occurrences of the Fe^{3+} dufrénite-group species are far more plentiful than those for Al species. There are well over 100 reported occurrences of dufrénite and natrodufrénite worldwide. Given the close similarity in appearance, properties, and cell parameters among the Fe^{3+} dufrénite-group species and the lack of chemical analyses for many reported occurrences, it is likely that gayite and possibly other new Fe^{3+} dufrénite-group species occur at other localities where they have been mistaken for dufrénite or natrodufrénite.

Acknowledgments

This study was funded, in part, by the John Jago Trelawney Endowment to the Mineral Sciences Department of the Natural History Museum of Los Angeles County. F. Colombo acknowledges the financial support of CONICET for a stay at Spain, where part of this research was conducted. We are grateful to Daniel Atencio and Stuart Mills for their comments that improved the manuscript.

References cited

Atencio, D., Coutinho, J.M.V., Mascarenhas, Y.P., and Ellena, J.A. (2006) Matioliite, the Mg-analog of burangaite, from Gentil mine, Mendes Pimentel, Minas Gerais, Brazil, and other occurrences. American Mineralogist, 91, 1932–1936.

Baldo, E.G.A. (1992) Estudio petrológico y geoquímica de las rocas ígneas y metamórficas entre Pampa de Olaen y Characato, extremo norte de la Sierra Grande de Córdoba. Córdoba. República Argentina, 294 p. Ph.D. thesis (unpublished), Universidad Nacional de Córdoba.

Brese, N.E. and O'Keeffe, M. (1991) Bond-valence parameters for solids. Acta Crystallographica, B47, 192–197.

Ferraris, G. and Ivaldi, G. (1988) Bond valence vs. bond length in O···O hydrogen bonds. Acta Crystallographica, B44, 341–344.

Fontan, F., Pillard, F., and Permingeat, F. (1982) La natrodufrénite (Na,□)(Fe^{+++},Fe^{++})(Fe^{+++},Al)$_5(PO_4)_4(OH)_6\cdot 2H_2O$, une nouvelle espèce minérale du groupe de la dufrénite. Bulletin de Minéralogie, 105, 321–326.

Galliski, M.A. (1999) Distrito pegmatítico Punilla. In E.O. Zappettini, Ed., Recursos Minerales de la República Argentina. Instituto de Geología y Recursos Minerales. SEGEMAR, Anales, 35, 547–550.

Galliski, M.A. and Černý, P. (2006) Geochemistry and structural state of columbite-group minerals in granitic pegmatites of the Pampean Ranges, Argentina. The Canadian Mineralogist, 44, 645–666.

Hawthorne, F.C. (1998) Structure and chemistry of phosphate minerals. Mineralogical Magazine, 62, 141–164.

Hawthorne, F.C. and Grice, J.D. (1990) Crystal-structure analysis as a chemical analytical method: application to light elements. The Canadian Mineralogist, 28, 693–702.

Kampf, A.R., Colombo, F., Simmons, W.B., Falster, A.U., and Nizamoff, J.W. (2010) Galliskiite, $Ca_4Al_2(PO_4)_2F_8\cdot 5H_2O$, a new mineral from the Gigante granitic pegmatite, Córdoba province, Argentina. American Mineralogist, 95, 390–394 (this issue).

King, P.L., White, A.J.R., Chappell, B.W., and Allen, C.M. (1997) Characterization and origin of aluminous A-type granites from the Lachlan Fold Belt, southeastern Australia. Journal of Petrology, 38, 371–391.

Latorre, C.O., Hurtado, A.E., and de Ponti, M.E.V. (1990) Mineralogía de la pegmatita El Gigante, Tanti, Córdoba, República Argentina. Apatita, granate y triplita. Revista de la Asociación Argentina de Mineralogía, Petrología y Sedimentología, 21, 33–36.

Lira, R. and Kirschbaum, A. (1990) Geochemical evolution of granites from the Achala Batholith of the Sierras Pampeanas, Argentina. In S.M. Kay and C.W. Rapela, Eds., Plutonism from Antarctica to Alaska, 241, p. 67–76. Geological Society of America, Special Paper, Boulder, Colorado.

Mandarino, J.A. (1981) The Gladstone-Dale relationship: Part IV. The compatibility concept and its application. The Canadian Mineralogist, 19, 441–450.

Martino, R.D. (2003) Las fajas de deformación dúctil de las Sierras Pampeanas de Córdoba: Una reseña general. Revista de la Asociación Geológica Argentina, 58, 549–571.

Moore, P.B. (1970) Crystal chemistry of the basic iron phosphates. American Mineralogist, 55, 135–169.

——— (1973) Pegmatite phosphates: Descriptive mineralogy and crystal chemistry. Mineralogical Record, 4, 103–130.

——— (1982) Pegmatite minerals of P(V) and B(III). In P. Černý, Ed., Granitic Pegmatites in Science and Industry, 8, p. 267–291. Mineralogical Association of Canada, Short Course Handbook, Québec.

Rapela, C.W., Baldo, E.G.A., Pankhurst, R., and Fanning, C.M. (2008) The Devonian Achala batholith of the Sierras Pampeanas: F-rich, aluminous A-type granites. VI South American Symposium on Isotope Geology, Expanded abstract of 8 pages (CD), San Carlos de Bariloche.

Selway, J.B., Cooper, M.A., and Hawthorne, F.C. (1997) Refinement of the crystal structure of burangaite. The Canadian Mineralogist, 35, 1515–1522.

Sheldrick, G.M. (2008) SHELXL97—Program for the refinement of crystal structures. University of Göttigen, Germany.

Simmons, W.B., Webber, K.L., Falster, A.U., and Nizamoff, J.W. (2003) Pegmatology: Pegmatite Mineralogy, Petrology, and Petrogenesis, 176 p. Rubellite Press, New Orleans.

Whalen, J.B., Currie, K.L., and Chappell, B.W. (1987) A-type granites; geochemical characteristics, discrimination and petrogenesis. Contributions to Mineralogy and Petrology, 95, 407–419.

Manuscript received May 25, 2009
Manuscript accepted September 23, 2009
Manuscript handled by Hongwu Xu